

# Space Technology 7 –

## Micropropulsion and Mass Distribution

A. Carmain, C. Dunn, J. Ziemer  
 Jet Propulsion Laboratory, California Institute of Technology, 4800 Oak Grove Dr., Pasadena CA 91109  
 andrew.carmain@jpl.nasa.gov, 818-393-2960

V. Hruby, D. Spence, N. Demmons, T. Roy, R. McCormick, C. Gasdaska, J. Young, W. Connolly  
 Busek Co., Inc., 11 Tech Circle, Natick MA 07160  
 vhruby@busek.com, 508-655-5565

J. O'Donnell, F. Markley, P. Maghami, O. Hsu  
 NASA Goddard Space Flight Center, Greenbelt MD 20771  
 james.r.odonnell@gsfc.nasa.gov, 301-286-5531

*Abstract*— The NASA New Millennium Program Space Technology 7 (ST7) project will validate technology for precision spacecraft control. The ST7 Disturbance Reduction System (DRS) will contain new micropulsion technology to be flown as part of the European Space Agency's LISA (Laser Interferometer Space Antenna) Pathfinder project. After launch into a low Earth orbit in early 2010, the LISA Pathfinder spacecraft will be maneuvered to a halo orbit about the Earth-Sun L1 Lagrange point for operations. The DRS will control the position of the spacecraft relative to a reference to an accuracy of one nanometer over time scales of several thousand seconds. To perform the control the spacecraft will use a new colloid thruster technology. The thrusters will operate over the range of 5 to 30 micro-Newtons with precision of 0.1 micro-Newton. The thrust will be generated by using a high electric field to extract charged droplets of a conducting colloid fluid and accelerating them with a precisely adjustable voltage. The control position reference will be provided by the European LISA Technology Package, which will include two nearly free-floating test masses. The test mass position and attitude will be sensed and adjusted using electrostatic capacitance bridges. The DRS will control the spacecraft position with respect to one test mass while minimizing disturbances on the second test mass. The dynamic control system will cover eighteen degrees of freedom, six for each of the test masses and six for the spacecraft. In the absence of other disturbances, the test masses will slowly gravitate toward local concentrations of spacecraft mass. The test mass acceleration must be minimized to maintain the acceleration of the enclosing drag-free spacecraft within the control authority of the micropropulsion system. Therefore, test mass acceleration must be predicted by accurate measurement of mass distribution, then offset by the placement of specially shaped balance masses near each test mass. The acceleration is characterized by calculating the gravitational effect of over ten million modeled points of a nearly 500-kg spacecraft. This paper provides an overview of the mission technology

and the process of precision mass modeling of the DRS equipment.<sup>1 2</sup>

### TABLE OF CONTENTS

TABLE OF CONTENTS.....	1
INTRODUCTION.....	1
TEST MASS ASSEMBLIES.....	2
INTEGRATED AVIONICS UNIT.....	3
DYNAMIC CONTROL SYSTEM.....	3
COLLOIDAL MICROTHRUSTERS.....	4
BUBBLE EFFECTS .....	7
MASS DISTRIBUTION - PURPOSE .....	8
MASS DISTRIBUTION - METHOD .....	8
ACKNOWLEDGEMENTS .....	9
REFERENCES.....	9
BIOGRAPHY.....	10

### INTRODUCTION

The ST7 project is based on the concept of a freely floating test mass contained within a spacecraft that shields the test mass from external forces. The test mass will ideally follow a trajectory determined only by the local gravitational field. The spacecraft position must be continuously adjusted to stay centered about the test mass — essentially, flying in formation with the test mass — to minimize changes in forces acting on the test mass due to the spacecraft itself. The ST7 system performance is characterized by the extent to which unwanted accelerations appear on the test mass and the accuracy with which the spacecraft is centered on the test mass. The project goals are to demonstrate position control to 100 nm<sup>2</sup>/Hz and propulsion system accuracy to 0.01 μN<sup>2</sup>/Hz over a frequency range of 1 mHz to 30 mHz.

In order to measure the level of accelerations appearing on the test mass, the test mass trajectory must be compared with a reference trajectory. The reference is provided by a second identical test mass located within the same instrument assembly. Being located in the same spacecraft, the second

<sup>1</sup> 1-4244-0525-4/07/\$20.00 ©2007 IEEE  
<sup>2</sup> IEEEAC paper #1608, Version 1, 7 Nov 2006

test mass must be controlled at frequencies below the measurement bandwidth to keep its position relative to the primary test mass, while being free of control forces within the measurement bandwidth to provide a reference for acceleration measurements. The position of the second test mass will be measured with respect to the spacecraft. To keep the second test mass as free from external disturbances as possible within the measurement bandwidth, the spacecraft attitude will be controlled to follow the motion of the second test mass in axes perpendicular to the line between the two test masses.

The functionality of the ST7 system is indicated in Figure 1. The two cubical test masses, provided by the European Space Agency [1], are tightly enclosed within housings rigidly attached to the body of the spacecraft. Electrodes on the inner faces of the housings are used to measure the position and orientation of the test masses with respect to the housings. This capacitive sensing mechanism has been used in many previous missions, including the Triad drag-free demonstration [2] and on Gravity Probe-B [3]. A laser interferometer will measure changes in distance between the two test masses to infer the residual acceleration noise. Colloidal microthrusters will be fired to oppose external forces, which are primarily due to solar radiation pressure acting on the spacecraft solar panel. The thrust will be continually adjusted to keep the spacecraft centered about the test masses.

In order to control the position of the spacecraft with an accuracy of  $100 \text{ nm}^2/\text{Hz}$ , the position of the test mass with respect to its housing will be measured with an accuracy of  $25 \text{ nm}^2/\text{Hz}$ , and the thrusters will have output controlled with a step size of  $0.1 \text{ } \mu\text{N}$  and a stability of  $0.01 \text{ } \mu\text{N}^2/\text{Hz}$ . The spacecraft attitude control accuracy, in rotation about the two axes perpendicular to the direction between the two test masses, is determined by the accuracy with which the position of the second test mass is measured divided by the distance between test masses, which is nominally 35 cm.

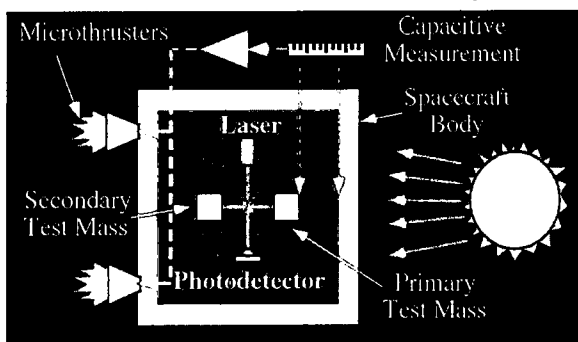


**Figure 1: Conceptual diagram of the ST7 Disturbance Reduction System.**

The use of the freely floating test masses as position and attitude references allows for a demonstration of the spacecraft control system to a high degree of accuracy. The test-mass control ensures that the spacecraft disturbances will be very low. For a separated-spacecraft interferometer mission, the control would be based on a spacecraft-spacecraft metrology system that is not included as part of the

DRS but could be used with the same thrusters and similar control algorithms to achieve a formation control at the nanometer level. For a single-aperture telescope, the microthrusters could be used with a pointing reference to provide a very stable attitude control.

For ST7, the key new technologies are the microthrusters and Dynamic Control Software. Busek Co., Inc, is developing the microthrusters. The NASA Goddard Space Flight Center is developing the control algorithms and software for adjustment of the spacecraft position and orientation. The European Space Agency is responsible for developing the test mass assemblies.

The ST7 equipment will be hosted on the European Space Agency LISA Pathfinder spacecraft. The European Space Agency is providing the test mass sensors to be used by ST7. The spacecraft will carry ST7 and related European experiment equipment to the Earth-Sun L1 Lagrange point for demonstration of the system capabilities. The mission duration is ninety days. The ST7 system elements are described below.

## TEST MASS ASSEMBLIES

### *Inertial Sensors – the Test Mass Housings*

The European Space Agency, together with its member states, is developing the test masses used for inertial sensing on the LISA Pathfinder mission [4]. The test mass will be a cube of low-magnetic-susceptibility, gold-platinum alloy that is 4.6 cm on a side and has a mass of approximately 2 kg. Each test mass is situated within a housing called an Inertial Sensor (IS). The separation between the test mass and its housing in all six degrees of freedom is monitored by non-contacting capacitor plates fixed to the housing. The capacitive walls can both measure and control the position and attitude of the test mass. For ST7, in order to reduce force noise from the measurement system acting on the test mass, the position readout requirements are  $25 \text{ nm}^2/\text{Hz}$ .

### *Disturbances*

The largest disturbances to the inertial trajectory of a spacecraft (radiation pressure, residual gas drag, and particulate impacts) are cancelled by the basic concept of a drag-reduction system. The final performance of the system will be limited by a number of smaller disturbances. These disturbances fall into three categories: 1) variations in the gravitational potential at the test-mass location, 2) momentum transfer to the test mass by residual gas and cosmic radiation particles, and 3) variations of the electromagnetic fields at the test-mass location. The main gravitational fluctuations are due to the thermal distortion of the spacecraft and to the relative displacement of the test mass with respect to the spacecraft. Reducing the gravity gradient and displacement of the test mass minimizes the gravity noise caused by spacecraft displacement. For reasonable space-experimental pressures,  $10^{-7} - 10^{-6} \text{ Pa}$  at 250 – 300 K, the forces caused by residual gas impacts are dominant compared to forces produced by cosmic radiation, though well below the requirement level. A number of electromagnetic effects cause test-mass disturbances; however, each can be minimized to a

considerable extent. Radiation-pressure differences across the gravitational sensor housing are reduced by thermal isolation and by making heat leaks as symmetrical as possible. Discharging the test-mass, reducing its displacement, and maximizing the test-mass-to-housing gap minimizes electric forces on the charged test mass. Fluctuating magnetic fields cause magnetic forces and, for a charged test mass, Lorentz forces. These forces are reduced by choosing a test-mass material with magnetic susceptibility of less than  $10^{-6}$  and by discharging the test mass. The residual charge on the test mass can be controlled by irradiating the test mass and housing with ultraviolet light, causing electrons to migrate to the more positively charged surface.

### INTEGRATED AVIONICS UNIT

The flight software resides on the Integrated Avionics Unit (IAU), which serves as the interface among the drag-free sensors, the thrusters, and the host spacecraft. Broad Reach Engineering is completing work on the IAU.

The IAU contains a 30-Mhz cPCI backplane, a Rad750 processor, and specialized cards to support communications with the spacecraft and the thrusters, as well as housekeeping sensor monitoring (temperature and currents). The IAU relays science data to the spacecraft, which is responsible for downlinking data to the ground.

The Dynamic Control Software also resides within the flight software. The flight software executes the DCS at 10 Hz. The spacecraft interface provides position and attitude measurements from the drag-free sensors, as well as the attitude and rates of the spacecraft. The DRS sends requested test mass forces and torques to the drag-free sensors. This supplements the force and torque commands sent to the colloid thrusters to act on the spacecraft.

### DYNAMIC CONTROL SYSTEM

#### *Test Mass Position and Attitude Control*

The spacecraft position and attitude are controlled with respect to the two test masses. One test mass must be controlled (suspended) with respect to the second (free) test mass at low frequencies to keep it within its reference

housing. The suspension force on the controlled test mass is exerted by applying control voltages to electrodes on the reference housing. This control force is a function of the position of the test mass within its housing, which couples motion of the spacecraft into a change in force on the test mass. In the absence of the control force, there would still, in general, be forces on the test masses that vary with the position of the spacecraft. One such coupling will arise from the gravitational force from the spacecraft components acting on the test masses (self gravity) that will be position dependent unless the mass is distributed with complete spherical symmetry.

Because of these coupling terms, the spacecraft motion with respect to the test mass needs to be minimized. The spacecraft position in each of three translation degrees of freedom can be controlled relative to the free test mass. The position of the suspended test mass is controlled (below the measurement band) in the direction of the free test mass using electrostatic suspension. The spacecraft attitude will be adjusted in two angular degrees of freedom to minimize motion of the spacecraft relative to the suspended test mass in the directions transverse to the direction between the test masses. The spacecraft will be controlled about the direction between test masses to keep the spacecraft solar panel pointed at the Sun. Each test mass will then be controlled in orientation to match the attitude of the spacecraft using electrostatically applied torques.

#### *Thrust Commanding*

The Dynamic Control System determines the thruster commands to control the spacecraft position and attitude based on the measurements of the position of each test mass relative to its housing. The variation in thrust commanded by DCS must be within the response capability of the thrusters. The magnitude of the thrust cannot exceed the electrostatic force capability of the housings. The electrostatic forces and torques for the test masses are a function of the test-mass housings. The spacecraft control requirement is to keep the spacecraft centered about the two test masses to less than  $100 \text{ nm}^2/\text{Hz}$  within the measurement frequency band of 1 mHz to 30 mHz.

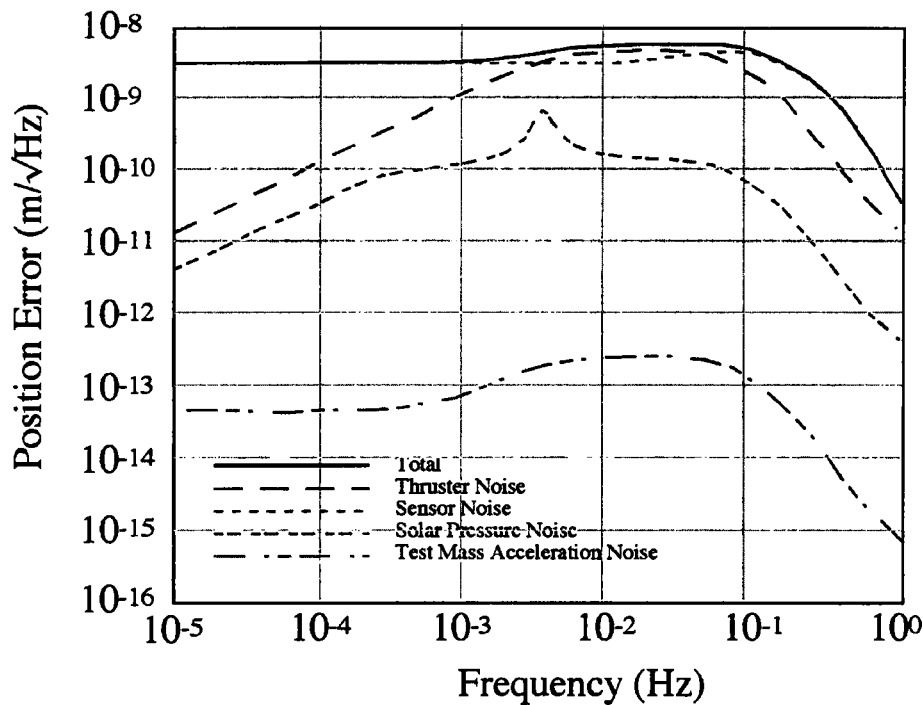


Figure 2: Power spectrum of simulated spacecraft control response for the position relative to the free test mass.

### Spacecraft Position and Attitude Control

The spacecraft position control requirements can be met with classical controller techniques, given the accurate position measurements of the test masses and the low level of thrust noise provided by the colloidal microthrusters. Figure 2 shows the power spectral behavior of a simulated system response for the position of the spacecraft with respect to the free test mass. The position control accuracy requirement is met throughout the measurement band. The position noise exhibits a slight increase near the controller unity gain frequency near 0.1 Hz. The selection of the crossover point represents a trade off between the controller update rate and the thruster dynamic range requirements. A higher controller update rate requires higher data and command transmission rates and lower data latencies, requiring high bandwidth and increased computation capability. A lower controller update rate results in larger variation in commanded thrust. An update rate of 10 Hz has been selected to be compatible with serial data transmissions while keeping thruster variations to 20% or less of nominal over time scales shorter than 1000 seconds.

Several disturbance models were included in the design of the controls: solar radiation pressure variation; capacitive sensing noise (modeled as a colored power spectrum); thruster and star tracker noise (modeled as white); and acceleration noise on the test mass, including magnetic and Lorentz forces, thermal variations (self gravity), and cosmic ray impacts.

### Monte Carlo Analysis

The stability of initial control is dependent on the initial conditions at handover of control from the spacecraft to DRS. A 10,000-run Monte Carlo of initial conditions showed that stable control for 99.6% of cases.

## COLLOIDAL MICROTHRUSTERS

### Thrust Requirements

The microthrusters must smoothly and continuously counter all external disturbances with control authority over all six degrees of freedom of the spacecraft motion. ST7 requires microthrusters capable of smoothly varying thrust from 5 to 30  $\mu\text{N}$  with 0.1- $\mu\text{N}$  resolution and temporal stability of  $0.01 \mu\text{N}^2/\text{Hz}$  for control of the position and attitude of the spacecraft. For ST7, the maximum thrust is determined by the need to counter the solar radiation pressure on the spacecraft, which is approximately 30  $\mu\text{N}$ . The thrust will be controlled with 0.1- $\mu\text{N}$  resolution in order to control the spacecraft position with respect to the reference (test mass) within  $100 \text{ nm}^2/\text{Hz}$ .

### Thruster System Overview

The ST7 microthrusters use a colloidal fluid propellant. The fluid is fed through a needle by a pressurizing system. At the tip of the needle, a high electrical field is applied, which causes droplets to form and to be ejected from the tip of the needle. The droplets are spontaneously charged and accelerated by the electric field.

A typical single-emitter-needle thruster produces a maximum thrust of 3  $\mu\text{N}$ . To achieve larger thrust, multiple needles are needed. For ST7 each thruster will use an array of 9 needles [5]. Measurements of thruster performance have been carried out and shown to meet performance requirements [6]. Four thrusters are mounted on one "cluster" assembly. Two clusters of thrusters will be used for ST7.

Each cluster consists of the thrusters, one carbon nanotube emitter, the propellant feed system, and the power-processing

unit (PPU). The PPU contains all the DC-DC converters to power the system and the autonomous controls for the carbon nanotube field emission neutralizer. The full thruster cluster configuration is shown in Figure 3.

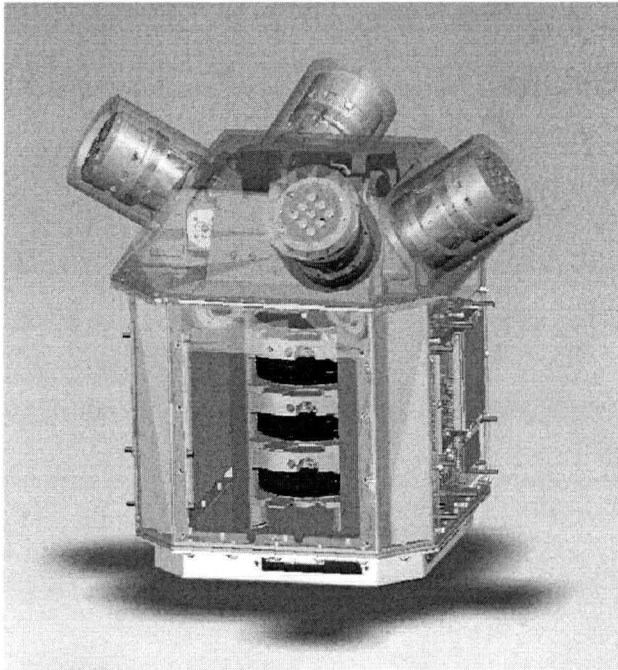


**Figure 3:** Design for ST7 colloid microthruster cluster, showing the four arrays of thruster needles (cylinders around the top) and the stack of propellant bellows in the thruster frame.

#### Propellant Feed System

The propellant is housed in flexible metal bellows in the center of the thruster frame. There is one bellows for each array of needles, called a “thruster assembly”, for a total of four bellows per cluster. Each bellows contains between 100 to 200 grams of propellant, sized to meet expected lifetime requirements with adequate margin. The four-bellows stack is under compression from constant-force springs. The arrangement of the bellows stack is shown in Figure 4.

The flow rate to the emitting needles is controlled with a piezotransducing microvalve, shown in Figure 5. The valve voltage is one variable used to control the thrust; others are discussed below. The valve allows very precise control of the flow rate and, thus, thrust. Figure 6 shows data from commanding the valve in step increments of 1 nA, with each step held for 30 seconds. This corresponds to a flow rate of 150 nL/min, or 2.5 nL/s.

After passing through the valve, heaters maintain the propellant at a stable temperature prior to ejection at the thruster needles.

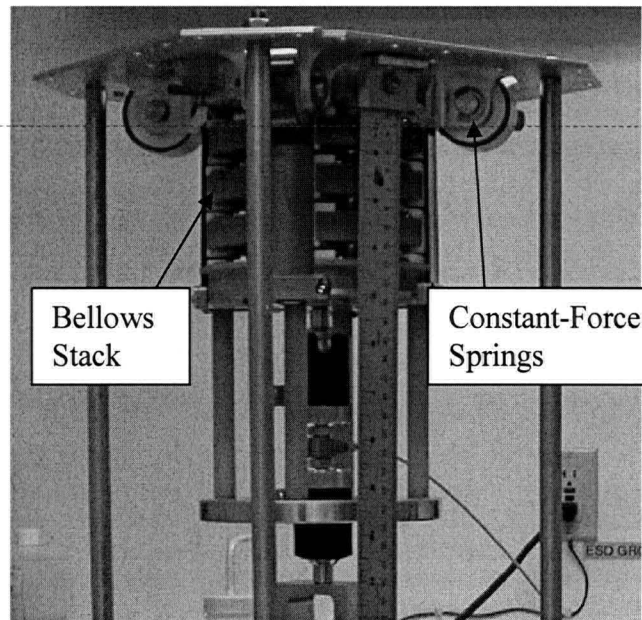


**Figure 4:** The stack of four bellows, compressed by constant-force springs.

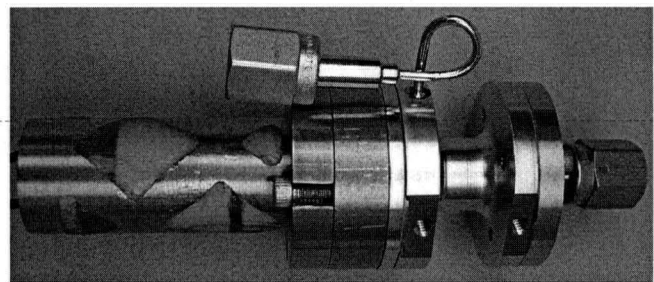


**Figure 5:** A piezo transducing microvalve provides precise flow control.

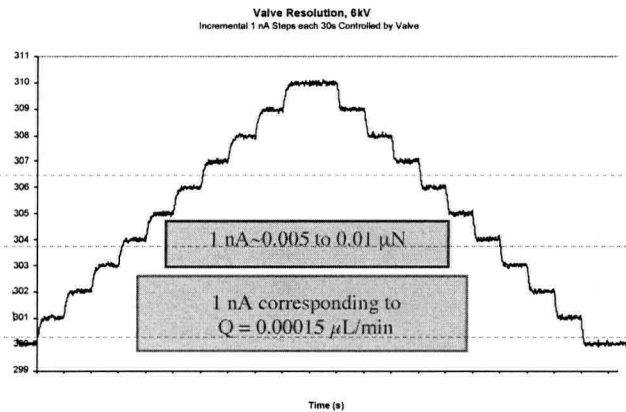


**Figure 6:** Demonstrates the 1 nA resolution of the thruster micro-valve. This corresponds to a flow rate of 150 nL/min, or 2.5 nL/s.

### Thruster Needles

Figure 7 shows a functional diagram of a typical microthruster needle. In general, the smaller the tube diameter the better; note, however, that practical considerations limit the tube inner diameter to some tens of microns. The propellant is relatively nonvolatile to minimize its evaporation when exposed to the vacuum of space and has a high electrical conductivity. When sufficient voltage is applied between the extractor and the microtube (emitter), the liquid surface deforms into a cone, as sketched in Figure 7. Taylor [7] found that this cone has a fixed angle of  $49.3^\circ$ , regardless of the type of fluid, its exact properties, or emitter geometry. Equilibrium on the surface of the cone is maintained by the balance of the liquid surface tension and electrostatic pressure. Near the tip, the electric field intensifies to a value that cannot be counteracted by the surface tension, and the cone tip transitions into a small-diameter jet of charged droplets, which are accelerated to produce thrust.

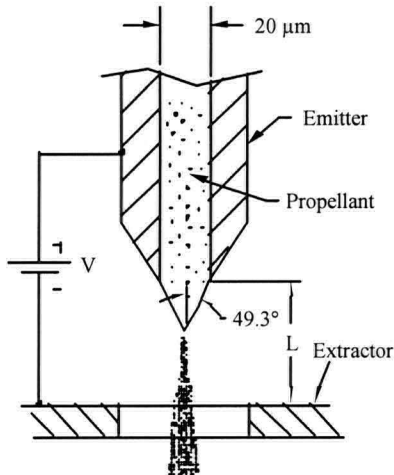


Figure 7: Schematic of the basic elements of a colloid thruster. A Taylor cone forms at the tip of the emitter upon application of sufficient voltage between the emitter and the extractor.



Figure 8: A thruster assembly, including the array of nine colloid thruster needles and the thruster heater at the opposite end.

### Neutralization

In order to prevent the spacecraft from becoming negatively charged by the continual ejection of positively charged droplets, the microthrusters include a carbon-nanotube cathode to emit electrons to keep the spacecraft neutral. The neutralizer appears alone in Figure 9, and depicted in place on the thruster in Figure 10.

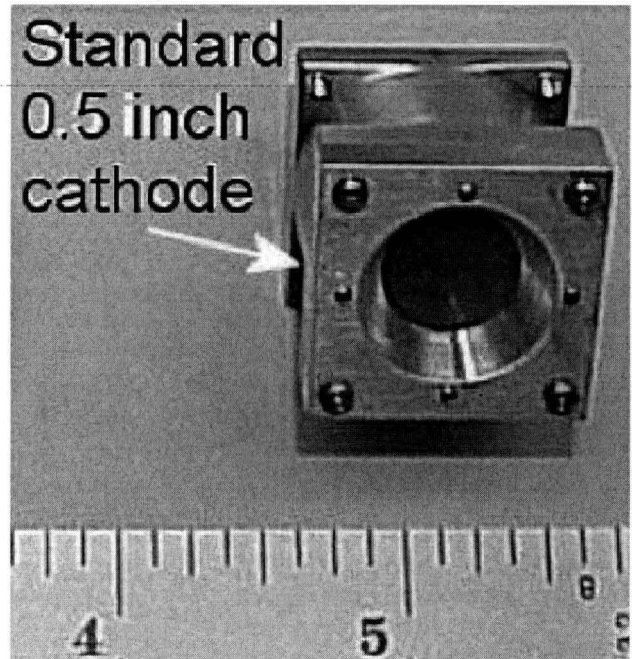


Figure 9: The 0.5" carbon nanotube cathode neutralizer.

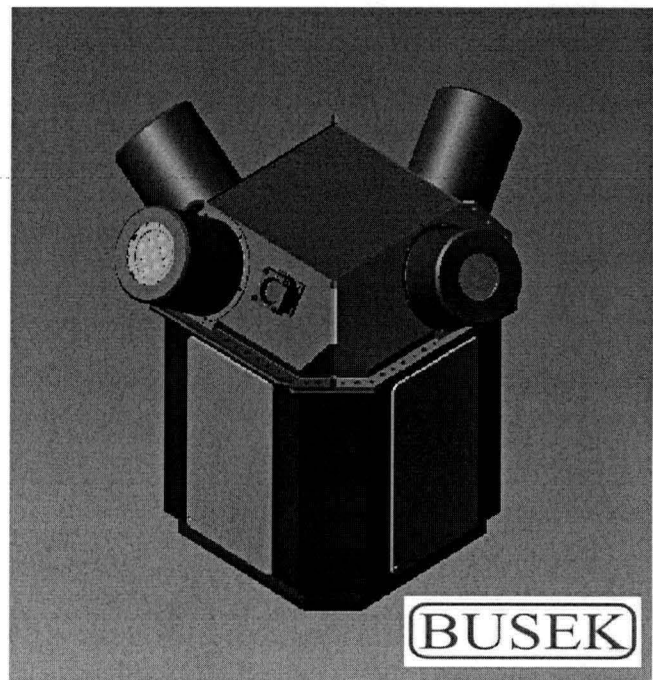


Figure 10: Location of the neutralizer on the thruster cluster.

### Thrust Control

In addition to the microvalve voltage, the dominant remaining variables to control thrust are the voltages of the emitter (at

the needle tip) and the extractor plate, which is offset from the emitter a short distance. Finally, the propellant is accelerated through a larger potential difference as it is ejected from the

assembly. The relative voltages greatly influence the thrust produced. Figure 11 shows the various voltages required to control the thrust.

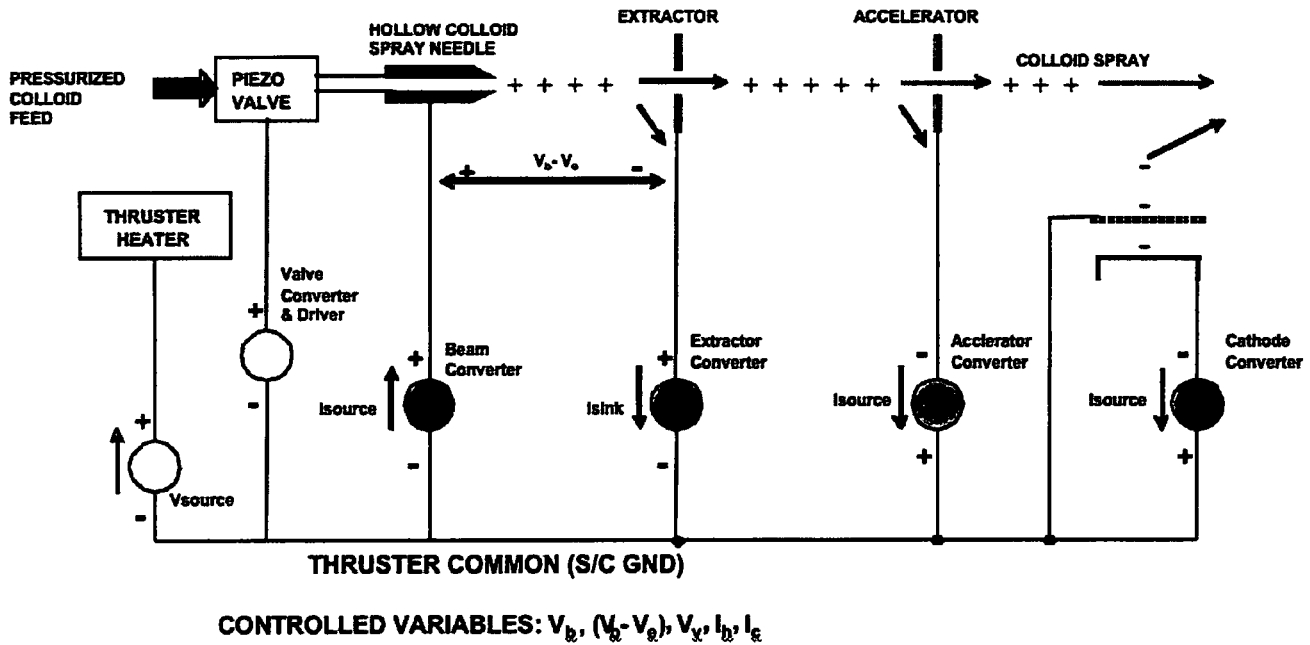


Figure 11: Control Voltages in the thruster system.

Typical thrust produced by a six-needle system is shown in Figure 12. Because the thrust may be varied through the action of the microvalve or the accelerating voltages, a level of control over the specific impulse is provided.

#### Bubble Effects

The hydrophilic propellant absorbs water and other gasses as it is handled in the lab environment and the bellows are filled. In operation, these gasses come out of solution as the propellant pressure drops in the feed system. These bubbles cause three problems during operation.

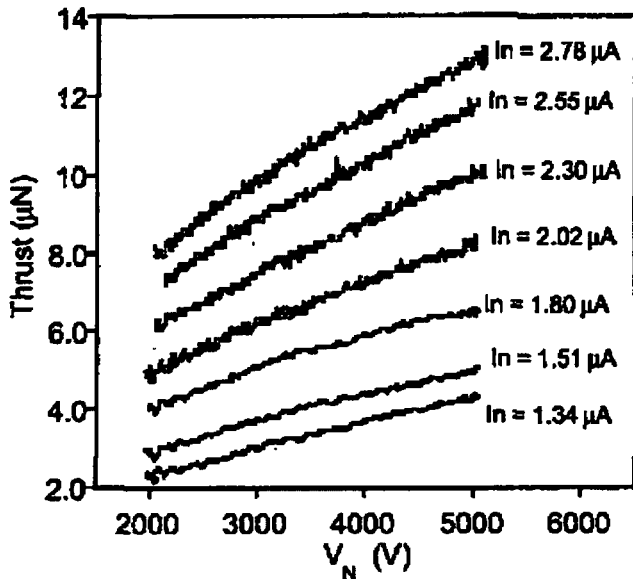


Figure 12: Thrust generated by the electrospray source as a function of emitter voltage and beam current (or propellant flow rate). Data shown for a six-needle thruster. [10]

The first problem is "overspray". On reaching the end of the emitter, the water rapidly expands and ejects propellant out of the needle at a lower charge to mass ratio than the droplets resulting from Taylor cone emission. The propellant, instead of traveling with the field and exiting the thruster, is deflected and lands on the extraction grid surface. This is termed "overspray". From the extraction grid, the propellant will wick and flow along the thruster surfaces. Eventually, when enough propellant has accumulated, it forms a conductive bridge between two surfaces of unequal potential - resulting in an electrical short of the thruster, thus preventing thrust and potentially damaging the thruster.

The second manner in which these bubbles interfere is due to their compressibility: the bubbles act as a capacitor in the feed system. The microvalve position is continuously varied to control thrust. As the valve position is changed, the dynamic pressure downstream of the valve changes, and the water bubbles compress or expand. Downstream at the emitter tips, there is a lag to the responding pressure drop. This effect is termed "compliance". As the valve is opened, the pressure from the bellows overwhelms the bubbles and the system pressure stabilizes quickly. Hence the response lag is small as the valve is opened. However, after the valve is closed and the bellows pressure goes to zero, the small bubbles continue

to expand gradually as they work against the hydraulic resistance in the feed system. This results in a slow leak at the emitter for a period after the valve has been closed, which causes thrust exceeding the commanded level.

Finally, bubbles in the feed system can block the small emitter passages. This results in the remaining emitter needles having to carry more current to provide a given thrust level. This higher than nominal current results in a greater level of overspray, with the attendant problems.

“Bubble eliminators” reduce the number of bubbles in the system. These are semi-permeable membranes placed downstream of the microvalve that allow gas bubbles to vent to space. Though effective, the bubble eliminators do not remove all bubbles from the system. Other bubbles pass through the emitter, causing hiccups in the delivered thrust. The frequency of these hiccups is initially as high as two per hour but drops with operating time.

The thruster performance with respect to bubble effects is measured by the response lag induced by the compliance. The instituted standard is the time required to change between maximum and minimum thrust. The response lag to the valve closing – decay time – is 85 seconds, while the response to the valve opening – rise time – is usually 1/10 of the closing time, 8.5 seconds.

However, bubble-induced compliance drops with operating time. After approximately 500 hours of operation, the decay time lowered and stabilized at 2-3 seconds. One option under consideration is to operate the thrusters on the ground for this “burn-in” period prior to delivery and installation on the spacecraft. We may also conduct such a burn-in during instrument commissioning on orbit, operating the thrusters at a net zero thrust level. This will allow the thruster to begin the mission with minimal bubbles. A burn-in prior to spacecraft installation will allow us to replace some of the expended propellant. The duration of the burn-in is limited by the preference to minimize operating time on the thrusters prior to on-orbit operations.

#### *Thruster Performance*

This compliance data is based on results from a single test unit. The flight units will be assembled and handled with improved procedures, developed with the intent of minimizing bubbles. Hence, the compliance of the flight units should be superior.

While the observed decay time meets the NASA mission requirement of 100 seconds, a faster response would allow the system to handle more dynamic environments. Beyond improved assembly procedures, we expect the compliance during flight operations to be much better than these lab results for other reasons. The flight environment contains more opportunities - time and vibration - for bubbles to escape from the feed system. Launch vibration will likely dislodge many bubbles from recesses. Subsequent to launch,

the thrusters will have several weeks in vacuum prior to first use, versus immediate use in the lab after evacuating the test chamber.

This design configuration has successfully completed long duration testing. The thruster under test fired continuously for 1.5 times mission lifetime, a total of 2200 hours. The test was extended and finally stopped after 3300 hours of successful operation.

### **MASS DISTRIBUTION - PURPOSE**

In addition to responding to external gravitational fields and gravitational waves, the test masses which form the heart of future gravitational wave detectors respond to the self-gravity resulting from the enclosing spacecraft. This self gravity presents several problems. If left unchecked, the test masses would eventually contact the enclosing spacecraft. To prevent this, a DC electrostatic force can be introduced which counters the effect of self-gravity or the drag-free control system can move the spacecraft to follow the DC component of the test-mass motion. Both alternatives are undesirable- the DC electrostatic force transmits mechanical noise from the spacecraft into the test mass, but chasing the DC component of the test mass motion uses thruster propellant and places demands on the thrust capability of the thrusters. Further, because LISA pathfinder and LISA contain two test masses, at least one must be electrostatically forced to follow the other.

Because of this quandary, it is necessary to adjust the local gravitational fields so that the DC gravitational force and force gradient are small. Because of the  $1/r^2$  force law it is possible to do this by placing high density materials near the test masses that compensate for the larger but more distant mass of the spacecraft.

To calculate the necessary shapes of the balance masses, we must first calculate the acceleration caused by the spacecraft itself, including its structure and all units onboard. Each instrument provider is required to provide mass distribution knowledge sufficient such that the uncertainty (that which cannot be balanced) in the differential acceleration is less than an allocated amount. For the DRS units, the requirement on the uncertainty is  $0.6e-10 \text{ m/s}^2$ . If the DRS consisted of 60 200-gram parts (just over 0.5 m from the test masses), a 5 mm error in the position of each part would consume the entire allocation of uncertainty. In actuality, DRS consists of many more parts of lower mass. Maintaining the mass and position of these parts and a useful estimate of the quality of the model has represented a significant challenge.

### **MASS DISTRIBUTION - METHOD**

Calculation of sufficient resolution for so many parts requires fairly exact knowledge of part mass and location.

To counter a common misconception, one cannot simply measure the center of gravity of a unit and calculate the gravitational acceleration from that. There is a significant difference between the center of gravity and the actual mass

distribution. An object can have two different mass distributions that would have the same center of gravity, but very different gravitational accelerations on a nearby point. The center of gravity calculation contains a linear weighting of mass from the point of interest, while the gravitational calculation contains an inverse quadratic relation.

Modeling methods vary for different types of masses: hard mechanical parts (chassis), soft mechanical components (cabling and plumbing), and electrical components (printed circuit boards). Each has a different degree of uncertainty in the location of its mass.

Hard mechanical parts are weighed easily and modeled by CAD programs as a set of discrete points. For homogenous parts, the error in mass and position will be quite low.

Soft mechanical parts can also be weighed easily, though their positions may not be known until installation onto the spacecraft. The routing of these soft goods can change the resulting gravitational field. We have measured the mass and length of the soft goods to calculate a linear density. From photographs of the equipment installed on hardware mockups, we identify positions of nodes along the length of the part. These positions are used to calculate the field for estimation, while the actual installed flight position may be slightly different. Any resulting differences must be measured on installation and factored into the data reduction. By this point of unit integration onto the spacecraft, it will be too late to modify the balance masses to account for the installed position.

Electronic components – circuit boards – actually carry the least knowledge of mass and location. Variations in mass occur from different length leads from standard mount components. The location on the boards is not as precise as mechanical parts because the electrical components may drift within the tolerance of the component pin holes or the size of the surface mount pads. Additionally, the distribution of staking and conformal coating is only estimated to be uniform, while concentrations for several possible reasons are ignored, deemed to be in the noise of the measurements.

#### ACKNOWLEDGEMENTS

The ST7 project is the result of large multi-institutional team whose work is summarized in the paper. The European Space Agency's LISA Pathfinder mission is managed by Giuseppe Racca. The colloid microthruster team at Busek Co., Inc. is led by V. Hruba and D. Spence. The Integrated Avionics Unit was designed and built by Broad Reach Engineering, under management of Scott Smader of Stanford University, and the Jet Propulsion Laboratory. The dynamic control system team at GSFC is led by J. O'Donnell, L. Markley, P. Maghami, and O. Hsu. The project management team is led by P. Barela and C. Dunn of JPL.

The research described in this paper was, in part, carried out by the Jet Propulsion Laboratory, California Institute of Technology, under a contract with the National Aeronautics and Space Administration.

#### REFERENCES

- [1] S Anza, M Armano, E Balaguer, M Benedetti, C Boatella, P Bosetti, D Bortoluzzi, N Brandt, C Braxmaier, M Caldwell, L Carbone, A Cavalleri, A Ciccolella, I Cristofolini, M Cruise, M Da Lio, K Danzmann, D Desiderio, R Dolesi, N Dunbar, W Fichter, C Garcia, E Garcia-Berro, A F Garcia Marin, R Gerndt, A Gianolio, D Giardini, R Gruenagel, A Hammesfahr, G Heinzl, J Hough, D Hoyland, M Hueller, O Jennrich, U Johann, S Kemble, C Killow, D Kolbe, M Landgraf, A Lobo, V Lorizzo, D Mance, K Middleton, F Nappo, M Nofrarias, G Racca, J Ramos, D Robertson, M Sallusti, M Sandford, J Sanjuan, P Sarra, A Selig, D Shaul, D Smart, M Smit, L Stagnaro, T Sumner, C Tirabassi, S Tobin, S Vitale, V Wand, H Ward, W J Weber and P Zweifel, "The LTP experiment on the LISA Pathfinder mission", *Classical and Quantum Gravity*, volume 22, pp S125-S138, 2004.
- [2] Space Science Dept of Johns Hopkins Applied Physics Laboratory and Guidance and Control Department of Stanford University, "A satellite freed of all but gravitational forces: Triad," *J. Spacecraft* 11, 637-644, 1974.
- [3] J. P. Turneaure, C. W. F. Everitt, B. W. Parkinson, *Advances in Space Research* 9, 29, 1989.
- [4] R Dolesi, D Bortoluzzi, P Bosetti, L Carbone, A Cavalleri, I Cristofolini, M DaLio, G Fontana, V Fontanari, B Foulon, C D Hoyle, M Hueller, F Nappo, P Sarra, D N A Shaul, T Sumner, W J Weber and S Vitale, "Gravitational Sensor for LISA and its Technology Demonstration Mission", *Class. Quantum Grav.* 20, 2003, S99-S108.
- [5] M. Gamero-Castaño and V. Hruba, "Electrospray as a source of nanoparticles for efficient colloid thrusters," *Journal of Propulsion and Power* 7, 977-987, 2001.
- [6] M. Gamero-Castaño and V. Hruba, "A torsional balance that resolves sub-micro-Newton forces," 27th International Electric Propulsion Conference, Pasadena, CA, 15-19 October 2001.
- [7] G.I. Taylor, "Disintegration of water drops in an electric field," *Proc. R. Soc., London A* 280, 383-397, 1964.
- [8] P. G. Maghami, O. C. Hsu, F. L. Markley, J. R. O'Donnell, Jr., "Control Modes of the ST7 Disturbance Reduction System Flight Validation Experiment," International Society for Optical Engineering Conference, San Jose, CA, 18-22 January 2004.
- [9] W. M. Folkner, "Space Technology 7 Disturbance Reduction System," 30th Government Microcircuit Applications and Critical Technology Conference, Las Vegas, NV, 4-7 April, 2005.
- [10] M. Gamero-Castaño, "Characterization of a Six-Emitter Colloid Thruster Using a Torsional Balance", *Journal of Power and Propulsion*, Vol. 20, No. 4, 2004.

## **BIOGRAPHY**

Andrew Carmain is a systems engineer on the ST7 project. He previously worked for United Space Alliance in the Mission Operations Training Group at Johnson Space Center. He received a B.S. in Aerospace Engineering from the University of Colorado, and a M.S. in Aeronautics & Astronautics from Stanford University.

End of File

